

A Journal of the Gesellschaft Deutscher Chemiker

# Angewandte Chemie

GDCh

International Edition

[www.angewandte.org](http://www.angewandte.org)

## Accepted Article

**Title:** Solid-Liquid-Gas Three-Phase Indirect Electrolysis Enabled by Affinity Auxiliary Imparted Covalent Organic Frameworks

**Authors:** Yi-Rong Wang, Ming Yue, Gang Liu, Jia-Li Zhang, Qi Li, Jing-Wen Shi, Jia-Yong Weng, Run-Han Li, Yifa Chen, Shun-Li Li, and Ya-Qian Lan

This manuscript has been accepted after peer review and appears as an Accepted Article online prior to editing, proofing, and formal publication of the final Version of Record (VoR). The VoR will be published online in Early View as soon as possible and may be different to this Accepted Article as a result of editing. Readers should obtain the VoR from the journal website shown below when it is published to ensure accuracy of information. The authors are responsible for the content of this Accepted Article.

**To be cited as:** *Angew. Chem. Int. Ed.* **2024**, e202413030

**Link to VoR:** <https://doi.org/10.1002/anie.202413030>

# Solid-Liquid-Gas Three-Phase Indirect Electrolysis Enabled by Affinity Auxiliary Imparted Covalent Organic Frameworks

Yi-Rong Wang<sup>[a]†</sup>, Ming Yue<sup>[a]†</sup>, Gang Liu<sup>[b]†</sup>, Jia-Li Zhang<sup>[a]</sup>, Qi Li<sup>[a]</sup>, Jing-Wen Shi<sup>[a]</sup>, Jia-Yong Weng<sup>[a]</sup>, Run-Han Li<sup>[a]</sup>, Yifa Chen<sup>[a]\*</sup>, Shun-Li Li<sup>[a]</sup> & Ya-Qian Lan<sup>[a]\*</sup>

[a] Dr. Y.-R. W., M. Y., J.-L. Z., Q. L., J.-W. S., J.-Y. W., R.-H. L., Prof. Y. C., Prof. S.-L. L., and Prof. Y. -Q. L. Guangdong Provincial Key Laboratory of Carbon Dioxide Resource Utilization, School of Chemistry, South China Normal University, Guangzhou, 510006, P. R. China  
E-mail: [chyf927821@163.com](mailto:chyf927821@163.com); E-mail: [yqlan@m.scnu.edu.cn](mailto:yqlan@m.scnu.edu.cn);

[b] G. L. State Key Laboratory of Heavy Oil Processing, College of Chemical Engineering, China University of Petroleum (East China) Qingdao, Shandong, 266580, P. R. China.

\*These authors contributed equally to this work.

Supporting information for this article is given via a link at the end of the document.

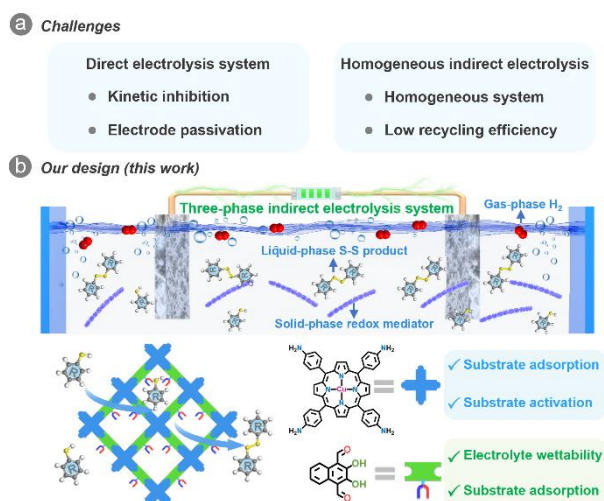
**Abstract:** The design of efficient heterogenous redox mediators with favorable affinity to substrate and electrolyte are much desired yet still challenging for the development of indirect electrolysis system. Herein, for the first time, we have developed a solid-liquid-gas three-phase indirect electrolysis system based on a covalent organic framework (Dha-COF-Cu) as heterogenous redox mediator for S-S coupling reaction. Dha-COF-Cu with the integration of high porosity, nanorod morphology, abundant hydroxyl groups and active Cu sites is much beneficial for the adsorption/activation of thiols, uniform dispersion and high wettability in electrolyte, and efficient interfacial electron transfer. Notably, Dha-COF-Cu as solid-phase redox mediator exhibits excellent electrocatalytic efficiency for the formation of value-added liquid-phase S-S bond product (yields up to 99%) coupling with the generation of gas-phase product of H<sub>2</sub> (~1.40 mmol g<sup>-1</sup> h<sup>-1</sup>), resulting in a powerful three-phase indirect electrolysis system. This is the first work about COFs that can be applied in three-phase indirect electrolysis system, which might promote the development of porous crystalline materials in this field.

## Introduction

Organic electrosynthesis using renewable electricity as energy source are widely recognized as efficient and eco-friendly pathways for the production of value-added products.<sup>[1]</sup> They hold much promise in chemical conversion of natural abundant small molecules like H<sub>2</sub>O and CO<sub>2</sub> as well as more complex organic compounds.<sup>[2]</sup> Generally, organic electrosynthesis can be basically classified into two categories based on their reaction pathways: direct electrolysis and indirect electrolysis.<sup>[3]</sup> Among them, indirect electrolysis using an electrocatalyst as “redox mediator” to mediate the electron transfer process between electrode and reactants shows various advantages over direct electrolysis.<sup>[2b, 4]</sup> However, most of reported redox mediators in indirect electrolysis are based on homogeneous molecular catalysts,<sup>[5]</sup> which suffer from complicated product separation process and low recycling efficiency.<sup>[6]</sup> As comparison, the heterogeneous redox mediator can reduce the overpotential, eliminate kinetic inhibition, increase reaction selectivity and avoid electrode passivation.<sup>[7]</sup> Nevertheless, the exploration of heterogeneous electrocatalysts as redox

mediators are still at an early stage with some unresolved issues, such as: 1) poor substrate adsorption and activation ability due to the lack in porosity of redox mediators; 2) low wettability of electrocatalyst with electrolyte that might inhibit the interfacial electron transfer; 3) lack in the microenvironment tuning of catalytic sites and systematic mechanism study. Thus, the design of efficient heterogeneous electrocatalysts to study the interface chemistry and catalytic microenvironment tuning is highly important for the development of novel indirect electrolysis systems.<sup>[6]</sup>

Covalent organic frameworks (COFs) are crystalline materials composed of organic repeating units with well-defined and designable porous structures.<sup>[8]</sup> COFs are ideal platforms to design heterogenous redox mediators for indirect electrolysis owing to the following reasons: 1) porous structures are beneficial for the substrate adsorption and activation;<sup>[9]</sup> 2) high-density and homogeneously dispersed active sites can serve as reaction platforms to catalyze the organic reactions;<sup>[10]</sup> 3) multiple functions can be introduced by the modification of organic construction struts with functional auxiliary, for example, enhanced interfacial wettability with electrolyte or affinity to substrates;<sup>[11]</sup> 4) tunable morphology and well-defined crystalline structure would be favorable for the electron transfer and mechanism study.<sup>[12]</sup> In this regard, it would be much interesting to design COFs based redox mediators to meet the high requirements of indirect electrolysis. Based on the evaluation of previously reported works, we intend to select copper- and hydroxyl group-based building blocks to contrast COFs for indirect electrolysis, and the relative considerations are listed as follows: 1) copper-based catalysts have been proven to be beneficial for the S-S coupling reaction; 2) hydroxyl groups would enhance the interfacial wettability of COFs with electrolyte and affinity with substrates. The combination of them might construct a desirable heterogenous platform to study the interface chemistry and catalytic microenvironment tuning, yet the applications of COFs in indirect electrolysis have not been demonstrated up to date and remain as an unexplored field.



**Scheme 1.** The schematic illustration of COFs as heterogeneous electrocatalysts to drive S-S coupling reaction in solid-liquid-gas three-phase indirect electrolysis system. (a) The challenges of conventional direct electrolysis system and homogeneous direct electrolysis system. (b) The solid-liquid-gas three-phase indirect electrolysis system.

As a proof-of-concept, for the first time, we have developed a solid-liquid-gas three-phase indirect electrolysis system based on a COFs (Dha-COF-Cu) as heterogeneous redox mediator for S-S coupling reaction (Scheme 1). Specifically, Dha-COF-Cu as solid-phase redox mediator presents excellent electrocatalytic efficiency for the liquid S-S bond products (yields up to 99%) and simultaneously generated gas product of  $H_2$  ( $\sim 1.40 \text{ mmol g}^{-1} \text{ h}^{-1}$ ). Besides, it enables the production of 10.01 g S-S bond product (i. e. 1,2-diphenyldisulfane) in a batch experiment. As proved by *in/ex-situ* characterizations and theoretical calculations, the hydroxyl groups as affinity auxiliary in Dha-COF-Cu can improve the wettability of COFs with electrolyte and promote the adsorption of substrate, thus possessing synergistic effect with Cu-porphyrin center to enhance the interfacial electron transfer and overall S-S coupling efficiency. This work offers a new strategy to design heterogeneous COFs electrocatalysts for three-phase indirect electrolysis system.

## Results and Discussion

Dha-COF-Cu and Naph-COF-Cu were synthesized via Schiff-base condensation between Cu-coordinated 5,10,15,20-tetrakis (4-aminophenyl)-porphyrato (TAPP-Cu) and 2,3-dihydroxynaphthalene-1,4-dicarbaldehyde (Dha) or naphthalene-1,4-dicarboxaldehyde (Naph) by solvothermal methods, respectively (details see Methods, Figure 1a). The powder X-ray diffraction (PXRD) and theoretical structural simulations were performed to define the crystalline structure of Dha-COF-Cu and Naph-COF-Cu (Figure 1b and Figure S1). The results show that Dha-COF-Cu possesses unit cell parameters of  $a = b = 33.9017 \text{ \AA}$ ,  $c = 3.0457 \text{ \AA}$ ,  $\alpha = \beta = \gamma = 90^\circ$ , using AA stacking model in  $P4$  space group with good residual factors of  $R_p = 2.28 \%$  and  $R_{wp} = 2.91\%$ , indicating the validity of computational model (Figure 1b). The peaks of PXRD pattern at

$3.74^\circ$  and  $7.22^\circ$  are assigned to the (1 1 0) and (2 2 0) planes, respectively. The simulated crystal structure of Dha-COF-Cu shows a one-dimensional channel with theoretical pore size of 1.92 nm, and the distance between adjacent layer is 3.04 Å (Figure 1a). In addition, Naph-COF-Cu is fitted into  $P4BM$  space group with unit cell parameters of  $a = b = 50.8482 \text{ \AA}$ ,  $c = 3.0013 \text{ \AA}$ ,  $\alpha = \beta = \gamma = 90^\circ$  ( $R_p$ , 3.46%;  $R_{wp}$ , 4.40%) (Figure S2). The chemical structures of Dha-COF-Cu and Naph-COF-Cu are further certified by Fourier transform infrared (FT-IR) spectra. Taking Dha-COF-Cu for instance, a new peak at  $1622 \text{ cm}^{-1}$  assigned to the C=N stretching vibration bond is observed, indicating the successful formation of C=N bonds. This result is further supported by the obviously decreased C=O stretching vibration ( $1700 \text{ cm}^{-1}$ ) and  $-NH_2$  vibration ( $3200\text{-}3500 \text{ cm}^{-1}$ ) that belong to the relative reactant monomers of Dha-COF-Cu (Figure S3).<sup>[13]</sup> Besides, compared with TAPP, the disappeared peak at  $3315 \text{ cm}^{-1}$  (N-H stretching vibration) and new peak at  $999 \text{ cm}^{-1}$  (Cu-N stretching vibration) confirm the metal coordination occurred at the porphyrin center (Figure S3). Similar results have also been detected for Naph-COF-Cu (Figure S4).<sup>[14]</sup> Thus, Dha-COF-Cu and Naph-COF-Cu have been successfully prepared for further study.

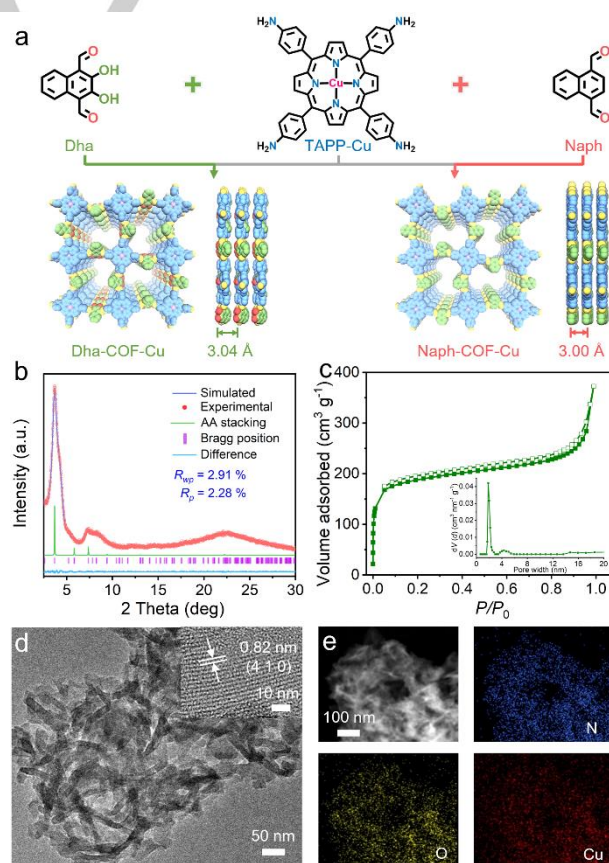


**Figure 1.** The preparation and characterization of Dha-COF-Cu and Naph-COF-Cu. (a) The scheme of the preparation of Dha-COF-Cu and Naph-COF-Cu. (b) Experimental and simulated PXRD patterns of Dha-COF-Cu. (c)  $N_2$  adsorption curve of Dha-COF-Cu at 77 K (inset shows the pore-size distribution profile). (d) The HRTEM image of Dha-COF-Cu. (e) STEM and mapping images of Dha-COF-Cu.



The surface area and porosity of Dha-COF-Cu and Naph-COF-Cu were detected by  $N_2$  sorption tests at 77 K (Figure 1c and Figure S5). In detail, the Brunauer-Emmett-Teller surface area ( $S_{BET}$ ) and total pore volume ( $V_t$ ) of Dha-COF-Cu are calculated to be  $593\text{ m}^2\text{ g}^{-1}$  and  $0.42\text{ cm}^3\text{ g}^{-1}$ , respectively (Figure 1c). The pore size distribution for Dha-COF-Cu basically complies with the theoretical results (Figure 1c). Besides, the  $S_{BET}$  and  $V_t$  of Naph-COF-Cu are calculated to be  $316\text{ m}^2\text{ g}^{-1}$  and  $0.25\text{ cm}^3\text{ g}^{-1}$ , respectively (Figure S5). Additionally, the chemical stability of Dha-COF-Cu and Naph-COF-Cu was confirmed by immersing them in different solvents at room temperature for more than 24 h. No obvious differences were observed in the PXRD patterns after the solvent treatment, demonstrating the well-remained crystalline structure and high chemical stability (Figure S6).

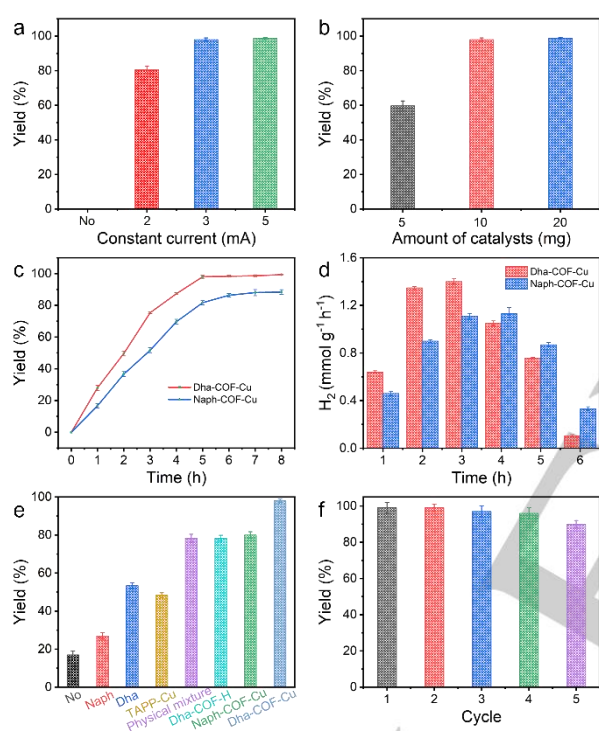


**Figure 2.** Indirect electrocatalytic performance of Dha-COF-Cu for S-S coupling. (a) The effect of current. Reaction conditions: carbon plate as anode, platinum plate as cathode, 10 mg catalyst, 5 h, **1** (0.25 mmol),  $n\text{-Bu}_4\text{NBF}_4$  (0.30 mmol),  $\text{CH}_3\text{CN}$  (6 mL), r.t. (b) The effect of catalyst amount. Reaction conditions: carbon plate as anode, platinum plate as cathode, constant current = 3 mA, 5 h, **1** (0.25 mmol),  $n\text{-Bu}_4\text{NBF}_4$  (0.30 mmol),  $\text{CH}_3\text{CN}$  (6 mL), r.t. (c) Time-dependent yield of **2a** for Dha-COF-Cu and Naph-COF-Cu. (d) Indirect electrocatalytic  $\text{H}_2$  evolution rate in S-S bond construction process. Reaction conditions for (c, d): carbon plate as anode, platinum plate as cathode, 10 mg catalyst, constant current = 3 mA, 8 h, **1** (0.25 mmol),  $n\text{-Bu}_4\text{NBF}_4$  (0.30 mmol),  $\text{CH}_3\text{CN}$  (6 mL), r.t. (e) Indirect electrocatalytic performance of Dha-COF-Cu and contrast samples. (f) The recycling experiment results. Reaction conditions for (e, f): carbon plate as anode, platinum plate as cathode, 10 mg catalyst, constant current = 3 mA, 5 h, **1** (0.25 mmol),  $n\text{-Bu}_4\text{NBF}_4$  (0.30 mmol),  $\text{CH}_3\text{CN}$  (6 mL), r.t.

Furthermore, the morphology of Dha-COF-Cu and Naph-COF-Cu were characterized by transmission electron microscopy (TEM) tests (Figure 1d and Figure S7). Dha-COF-Cu shows a kind of nanorod morphology while Naph-COF-Cu displays the nanosphere morphology (Figure 1d and Figure S7). In high-resolution TEM (HR-TEM) image, the directional lattice stripes of

the structural characteristics of Dha-COF-Cu were visualized and the lattice spacing of 0.82 nm can be attributed to the (4 1 0) crystalline plane of Dha-COF-Cu, suggesting its high crystallinity (Figure 1d). In addition, the energy-dispersive X-ray (EDS) elemental mapping images show that C, N, O, and Cu are uniformly distributed over Dha-COF-Cu and Naph-COF-Cu (Figure 1e and Figure S8). The electronic states of the elements in Dha-COF-Cu and Naph-COF-Cu were analyzed by X-ray photoelectron spectroscopy (XPS) characterization. The C 1s, N 1s, O 1s and Cu 2p signals are clearly detected in the XPS spectra of Dha-COF-Cu. In the Cu 2p region, two kinds of peaks with binding energy of 934.9 eV (Cu 2p<sub>3/2</sub>) and 954.7 eV (Cu 2p<sub>1/2</sub>) can be assigned to Cu (II) (Figure S9).<sup>[15]</sup> Similar results have also been detected for Naph-COF-Cu (Figure S10). The Cu content in Dha-COF-Cu and Naph-COF-Cu were tested to be 4.55% and 4.01% by inductively coupled plasma optical emission spectrometry (ICP-OES), which are in accordance with the results of EDS tests (Figure S11).

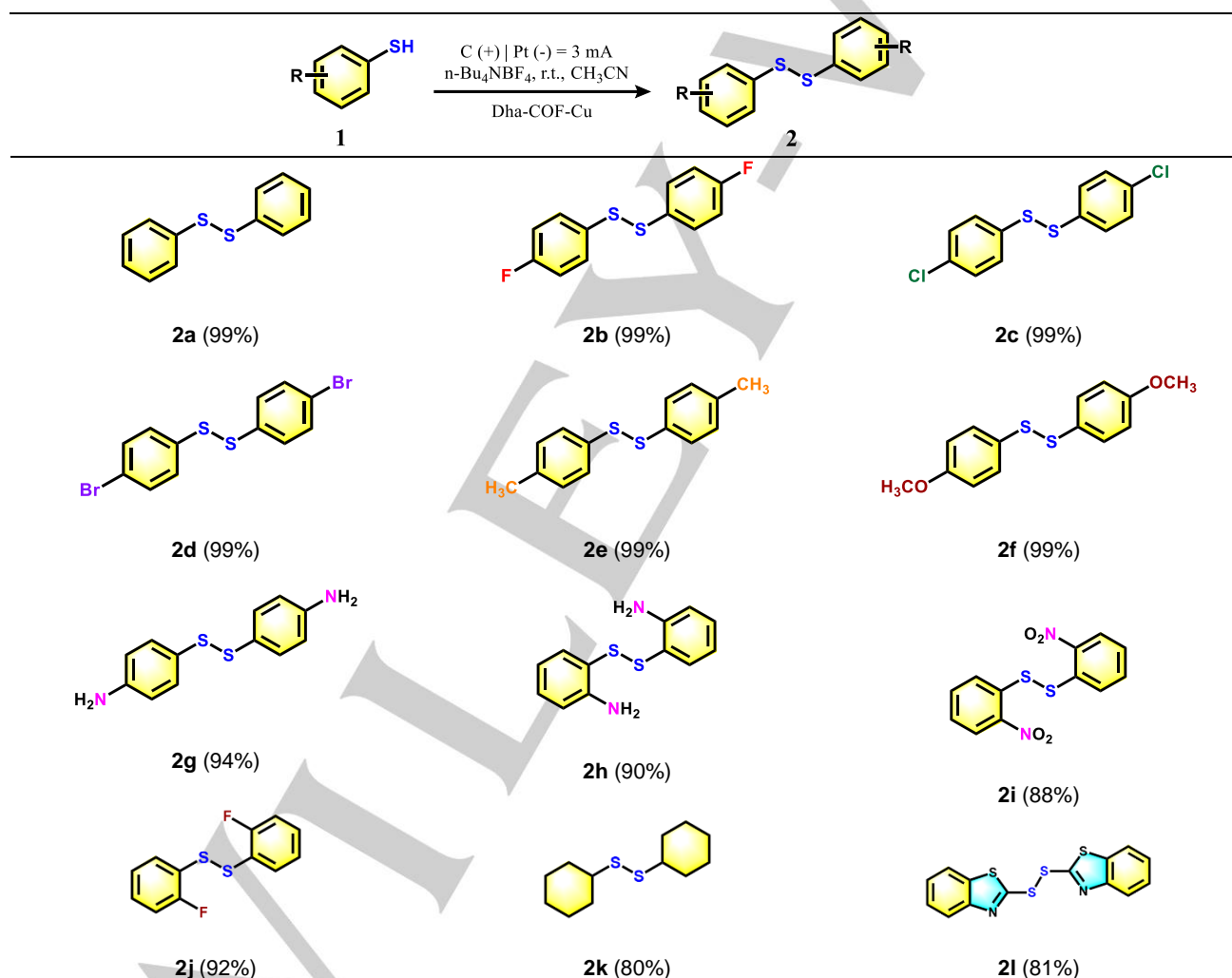
Symmetrical disulfides are vital structural motifs in pharmaceutical, biological science, natural compounds and advanced materials and so on.<sup>[6b, 6c, 7c]</sup> Compared to the conventional synthesis or direct electrolysis strategies with obstacles like side-reactions and separation problems, the solid-liquid-gas three-phase indirect electrolysis system based on COFs can simultaneously produce liquid-phase S-S products and gas-phase  $\text{H}_2$  in a single system, which would satisfy the requirements of green and sustainable synthesis. To study the possibility of these COFs in the indirect electrolysis system, the indirect electrocatalytic coupling reaction of benzenethiol (**1**) was initially selected as the S-S reaction model to explore the reaction conditions and Dha-COF-Cu was evaluated as catalyst (Figure S12). The product was monitored and quantified by mass spectra (MS) and gas chromatography (GC) (Figure S13-15). Initially, MeCN and  $n\text{-Bu}_4\text{NBF}_4$  were selected as the reaction solvent and electrolyte based on the reported work.<sup>[7a]</sup> Then, some contrast experiments using Dha-COF-Cu as catalyst were conducted to optimize the reaction conditions including reaction current, amount of catalyst, solvent, electrolyte, electrode and reaction voltage, etc. The effect of reaction current on indirect electrocatalytic S-S bond coupling was monitored and quantified at different currents. The result shows that the yield of **2a** (1,2-diphenyldisulfane) gradually enhances to the maximum yield of  $98\pm 1\%$  at 3 mA with the increasement of operation current and maintains almost unchanged performance at 5 mA current (Figure 2a). Besides, chronoamperometric and chronopotentiometric curves show that the electrocatalysis activity has no obvious change, indicating the high electrochemical stability during the reaction process (Figure S16). Additionally, the catalyst amount of Dha-COF-Cu was optimized in this system. With the addition of 5 mg catalyst, the yield of **2a** is  $59.6\pm 2.8\%$ . Then, the yield of **2a** increases to  $98\pm 1\%$  with 10 mg catalyst and has no significant improvement with 20 mg catalyst. Thus, 10 mg was selected as the desired amount of catalyst for further tests (Figure 2b and Table S1). Moreover, several kinds of solvents including  $\text{H}_2\text{O}$ , EtOH, or the mixture of MeCN and  $\text{H}_2\text{O}$  have been applied in indirect electrocatalytic S-S coupling reaction, yet none of them are beneficial to enhance the yield of **2a** (Figure S17). Then,  $n\text{-Et}_4\text{NBr}$  and  $n\text{-Bu}_4\text{NBr}$  were applied as replaced electrolytes of  $n\text{-Bu}_4\text{NBF}_4$ , yet they exhibit unsatisfactory results (Figure S18). These results indicate that MeCN (6 mL) and  $n\text{-Bu}_4\text{NBF}_4$  (0.3

mmol) are the optimal reaction solvent and electrolyte in the reaction system to deliver **2a** with a 98±1% yield. Further optimizations have been carried out by screening different electrodes, including C (+)-C (-), C (+)-Pt (-) and Pt (+)-Pt (-) to evaluate the practicality of indirect electrocatalytic S-S reaction (Figure S19). C (+)-Pt (-) was proved to be the optimized electrode to deliver the best performance of indirect electrocatalytic S-S coupling reaction.

To further evaluate the catalytic performance of Dha-COF-Cu for indirect electrocatalytic S-S reaction, the reaction yields at different time intervals were evaluated (Figure 2c). As a result, the yield of **2a** has a continuous growth as the reaction time increases and finally reaches up to 98±1% at 5 h (Figure 2c). With the increase of reaction time, the yield of **2a** has no

significant improvement. In comparison, the highest yield of **2a** for Naph-COF-Cu is 86±1% at 6 h (Figure 2c). In addition to the production of S-S bond product, the production of H<sub>2</sub> was also detected every 1 h during the reaction process (Figure 2d). The production rate of H<sub>2</sub> for Dha-COF-Cu gradually increases from 0.64 mmol g<sup>-1</sup> h<sup>-1</sup> at 1 h to maximum value of 1.40 mmol g<sup>-1</sup> h<sup>-1</sup> at 3 h (Figure 2d). In contrast, the production rate of H<sub>2</sub> for Naph-COF-Cu can reach up to 1.1 mmol g<sup>-1</sup> h<sup>-1</sup> at 3 h (Figure 2d). These results prove that the strategy of solid-liquid-gas three-phase indirect electrolysis system based on Dha-COF-Cu as heterogeneous redox mediator can simultaneously and efficiently produce S-S products and H<sub>2</sub> in a single system, which would be much beneficial for the separation of products and recovery of catalysts.

**Table 1.** Substrate scope of disulfides.<sup>a,b</sup>



<sup>a</sup>) Reaction conditions: carbon plate (53 mm \* 8 mm \* 1.5 mm) as anode, platinum plate (53 mm \* 8 mm \* 1.5 mm) as cathode, Constant current = 3 mA, 5 h, **1** (0.25 mmol), *n*-Bu<sub>4</sub>NBF<sub>4</sub> (0.30 mmol), CH<sub>3</sub>CN (6 mL), r.t.;

<sup>b</sup>) Isolated yields.

In addition, to confirm the superiority of Dha-COF-Cu for indirect electrocatalytic S-S reaction, some contrast samples have been tested (Figure 2e). Initially, Dha-COF-H (without

metal in porphyrin center) (78.3±1.5%) and TAPP-Cu (48.4±1.2%) exhibits lower yields of **2a** than that of Dha-COF-Cu (98±1%) in indirect electrocatalytic S-S reaction, suggesting the porphyrin-Cu to be an important catalytic unit in the reaction.

Besides, to support the vital role of hydroxyl group for Dha-COF-Cu, the performances of Naph, Dha and Naph-COF-Cu (i.e. none hydroxyl counterpart of Dha-COF-Cu) were evaluated. The results show that the Naph, Dha and Naph-COF-Cu can convert **1** to **2a** with low yield of  $27.0 \pm 1.7\%$ ,  $53.3 \pm 1.5\%$  and  $80.0 \pm 1.7\%$ , respectively. In addition, the physical mixture of Dha and TAPP-Cu displays a  $78.3 \pm 2.1\%$  yield of **2a**, demonstrating the superiority of well-defined porous structure in Dha-COF-Cu (Figure 2e). These results indicate that the porphyrin-Cu and hydroxyl group might play synergistic roles in enhancing the catalytic performance of indirect electrocatalytic S-S coupling reaction.

The persistence of catalytic performance is also a key factor for estimating the practicability of samples. To explore the stability of catalyst, the long-term and recycling tests of Dha-COF-Cu in indirect electrocatalytic S-S coupling reaction were further carried out using the model reaction under optimal conditions. As shown in Figure S20, the current can maintain stable during the process of 20 h stability test. For the recycling test, Dha-COF-Cu was easily separated after each recycling test, and then reused in the successive coupling reactions. Notably, no obvious deactivation is observed after 5 cycle tests (Figure 2f). Then, to characterize the structure stability of Dha-COF-Cu after indirect electrochemical process, the PXRD and FT-IR tests of Dha-COF-Cu were performed, in which the peaks are basically unchanged relative to the pristine sample (Figure S21, S22). Additionally, the XPS spectra of Dha-COF-Cu after recycling tests indicate that the binding energy of Cu species are consistent with the sample before test (Figure S23). Moreover, to evaluate the industrial applicability of indirect electrocatalytic synthesis, the scale-up synthesis of **2a** was carried out under optimal conditions. As a result, 10.01 g **2a** with a yield of  $\sim 82\%$  can be readily produced in a batch experiment (Figure S24). The above results imply that Dha-COF-Cu is a kind of stable electrocatalyst that can be applied for the scale-up production, holding much promise for the practical applications of indirect electrocatalytic S-S coupling reaction.

The scope and generality of indirect electrocatalytic S-S coupling reaction to construct symmetric disulfides have been explored and the outcomes are shown in Table 1. The benzenethiol bearing both electron-withdrawing (-F, -Cl and -Br) and electron-donating (-CH<sub>3</sub>, -OCH<sub>3</sub> and -NH<sub>2</sub>) substituents at para-position provides desired products in 94-99% yields (Table 1, **2b** - **2i**). Besides, 4-aminothiophenol and 2-nitrothiophenol deliver the corresponding S-S bond self-coupling products with 90% and 88% yield, which might be due to the large steric hindrance of ortho-substituted benzenethiol substrates in this reaction system. Moreover, 2-fluorothiophenol, cyclohexanethiol and 2-mercaptobenzothiazole supply desired products with 92%, 80% and 81% yields, respectively (**2j** - **2l**).

To unveil the transformation mechanism of **1** to **2a** under indirect electrocatalytic conditions, some control experiments were carried out. The results show that the desired products are not obtained without current under optimal conditions, indicating that the indirect electrocatalytic S-S self-coupling reaction could not proceed in the absence of the electric current (Figure 2a). Besides, the addition of radical scavenger 5,5-dimethyl-1-pyrroline N-oxide (DMPO) to the reaction system significantly inhibits the S-S self-coupling and no corresponding **2a** has not been detected under optimal conditions, suggesting the formation of S-S bond is a free radical mediated electrocatalytic

reaction system. Additionally, electron paramagnetic resonance (EPR) measurements with 5,5-dimethyl-1-pyrroline-N-oxide (DMPO) as the radical spin-trapping reagent were conducted to confirm the generation of thiol radicals during the reaction. The characteristic signal of EPR is not detected under without electricity condition, while the characteristic peak of thiol radicals is observed under electricity condition (Figure S25a). Besides, the coupling products of S and radical inhibitors was captured by HRMS spectrum (Figure S25b). These results confirm the generation of thiol radicals during the indirect electrocatalytic S-S coupling reaction.

Furthermore, the theoretical calculations were performed to support the distinction of the indirect electrocatalytic S-S coupling reaction performances. Initially, to investigate the extent of acetonitrile molecule wetting by Dha-COF-Cu and Naph-COF-Cu, we conducted a 2000 ps molecular dynamics simulation of samples in acetonitrile to approximate an equilibrium state (Figure 3a, Figure S26 and S27). The radial distribution function displays that the closest neighbor distribution of hydroxyl group's H in Dha-COF-Cu with acetonitrile is around 1.25 Å and 2.3 Å (Figure 3b). In contrast, the neighboring coordination of acetonitrile molecules with Naph-COF-Cu is much lower, suggesting that Dha-COF-Cu has better affinity with acetonitrile.

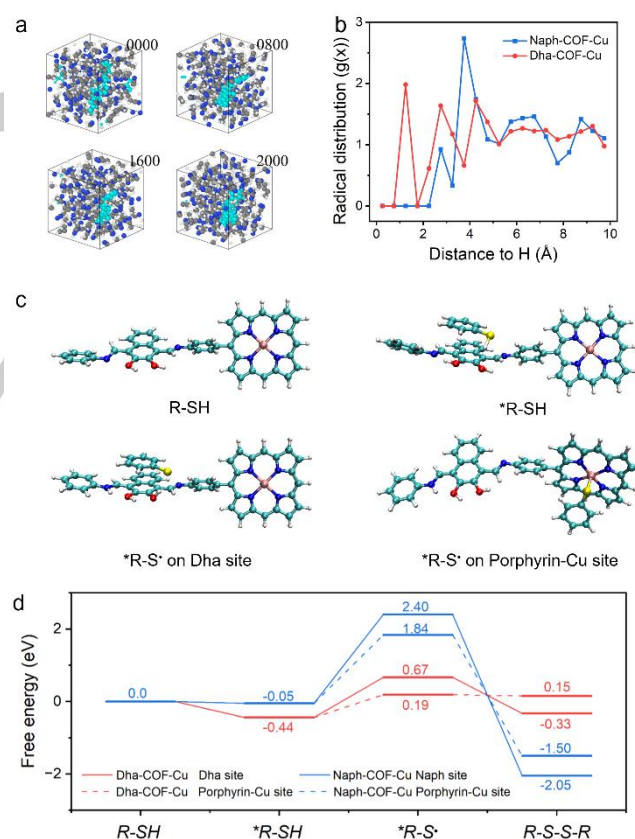


**Figure 3.** DFT calculations of Dha-COF-Cu and Naph-COF-Cu for S-S coupling. (a) The radial distribution function of acetonitrile on Dha-COF-Cu and Naph-COF-Cu (represented by the nearest H atoms). (b) The geometric structure diagrams and independent gradient model based on Hirshfeld partition (IGMH) analysis of the benzenethiol adsorbed on the Dha-COF-Cu. (c) The geometric structure diagrams of the corresponding species on Dha-COF-Cu for S-S coupling. (d) Free energy profiles for S-S coupling reaction pathway without voltage on Dha-COF-Cu and Naph-COF-Cu (R-SH stands for benzenethiol).



To assess the contribution of hydroxyl groups in COFs to the adsorption of substrate, the adsorption energy ( $\Delta E_{ads}$ ) of benzenethiol (R-SH) on Dha-COF-Cu and Naph-COF-Cu was calculated by density functional theory (DFT) calculation (Figure S28). The results show that the  $\Delta E_{ads}$  of Dha-COF-Cu (-29.8 kcal/mol) is larger than that of Naph-COF-Cu (-13.6 kcal/mol), indicating a better adsorption ability of Dha-COF-Cu for benzenethiol. Besides, as revealed in the independent gradient model based on Hirshfeld partition (IGMH) analysis results,<sup>[16]</sup> stronger  $\pi$  conjugation interactions exist between Dha-COF-Cu and benzenethiol (Figure S28). There is obvious hydrogen bond interaction existed between the H atom of thiol and the O atom hydroxyl group of Dha-COF-Cu (Figure S28). In addition, the Wiberg bond order calculations show that the S-H bond order of Dha-COF-Cu (0.17) is lower than that of Naph-COF-Cu (0.24) and benzenethiol (0.97), demonstrating the bond energy of S-H bond in benzenethiol can be reduced by  $\pi$  conjugate interactions with Dha-COF-Cu (Figure S28). These results indicate that Dha-COF-Cu has a better adsorption and activation ability for the thiol substrates.

To further explore the mechanism of S-S coupling reaction, the potential energy surface is evaluated for the S-S coupling processes on Dha-COF-Cu and Naph-COF-Cu, respectively (Figure 3c, 3d, S29 and S30). The S-S coupling reaction is supposed to be realized by the coupling of two free  $\cdot R-S$  radicals, which is produced from the adsorption and activation of R-SH. The formation of  $\cdot R-S$  radicals is the rate-determining step in the S-S coupling process. As revealed in the DFT calculation results, the benzenethiol was firstly adsorbed on the surface of Dha-COF-Cu with a Gibbs free energy change ( $\Delta G^\circ$ ) value of -0.44 eV (Figure 3c, 3d). Then, the  $\cdot R-S$  radical was formed coupling with the proton-coupled electron transfer processes. In this process, two possible sites were calculated including Dha site and porphyrin-Cu site in Dha-COF-Cu. The results show that the  $\cdot R-S$  radical capture ability of porphyrin-Cu site ( $\Delta G^\circ = 0.63$  eV) is higher than that of Dha site ( $\Delta G^\circ = 1.11$  eV). Besides, due to the formation of new Cu-S bonds after porphyrin-Cu captures  $\cdot R-S$  radicals, the subsequent S-S coupling process needs to overcome the energy for bond breaking, resulting in slightly endothermic process relative to the zero point ( $\Delta G^\circ = 0.15$  eV). In contrast, the  $\cdot R-S$  at the Dha site remains as a free radical state, and the S-S coupling is calculated to be a spontaneous reaction step. Specifically, the potential determining step for the S-S coupling on Dha-COF-Cu is the formation of  $\cdot R-S$  with the potential of 1.11 V for Dha site and 0.63 V for porphyrin-Cu site, respectively (Figure 3d). Thus, this potential barrier can be completely conquered under a constant current of 3 mA (about 2 V potential), indicating that S-S coupling reaction can be achieved under the experiment condition (Figure 2e, 3d and S29). Similarly, the S-S coupling reaction on Naph-COF-Cu also undergoes the substrate adsorption, free radical generation, and S-S coupling pathways. As shown in Figure 3d, the formation of  $\cdot R-S$  has higher overpotential (Naph site, 2.45 V; porphyrin-Cu site, 1.89 V) on Naph-COF-Cu than that of Dha-COF-Cu (Figure 3d, S29 and S30). The above theoretical calculations can be well consistent with the catalytic performances of the experiments, further proving the synergistic effect of porphyrin-Cu and Dha sites on improving the wettability with electrolyte, adsorption of substrate and lower the energy barrier to boost overall S-S coupling efficiency.

## Conclusion

In summary, for the first time, a solid-liquid-gas three-phase indirect electrolysis system based on a COFs (Dha-COF-Cu) as heterogenous redox mediator for S-S coupling reaction has been developed. Notably, Dha-COF-Cu as solid-phase redox mediator presents excellent electrocatalytic efficiency for the liquid S-S bond products (yields up to 99%) and simultaneously generated gas product of  $H_2$  ( $\sim 1.40$  mmol  $g^{-1} h^{-1}$ ). Besides, it enables the scale-up production of 10.01 g S-S bond product (i.e. 1,2-diphenyldisulfane) in a batch experiment. Additionally, the hydroxyl groups as affinity auxiliary can improve the wettability of COFs with electrolyte and promote the adsorption of substrate, thus possessing synergistic effect with Cu-porphyrin center to enhance the interfacial electron transfer and overall S-S coupling efficiency as certified by *in/ex-situ* characterizations and DFT calculations. This work might shed light on the design of heterogenous catalysts for the advanced solid-liquid-gas three-phase indirect electrolysis systems.

Supplemental Information includes 42 figures and 1 table.

## Acknowledgements

This work was financially supported by the National Key R&D Program of China (2023YFA1507204). The National Natural Science Foundation of China (Grants 22225109, 22309054, 22171139, 22071109, 22371080, 22301084). China Postdoctoral Science Foundation (No. 2023M731154, No. 2023M741232). China National Postdoctoral Program for Innovative Talents (BX20220116). Guangdong Basic and Applied Basic Research Foundation (2024A1515013220). Natural Science Foundation of Guangdong Province (No. 2023B1515020076).

## Conflict of Interest

The authors declare no conflict of interest.

**Keywords:** COFs; Redox mediator; Three phase; Indirect electrolysis; S-S coupling reaction.

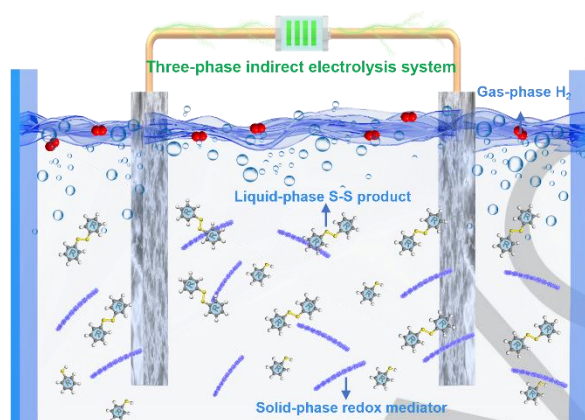
## References

- [1] a) M. Yan, Y. Kawamata, P. S. Baran, *Chem. Rev.* **2017**, *117*, 13230-13319; b) J. Liu, L. Lu, D. Wood, S. Lin, *ACS Central Science* **2020**, *6*, 1317-1340; c) E. J. Horn, B. R. Rosen, P. S. Baran, *ACS Central Science* **2016**, *2*, 302-308; d) L. Xu, Z. Huang, M. Yang, J. Wu, W. Chen, Y. Wu, Y. Pan, Y. Lu, Y. Zou, S. Wang, *Angew. Chem. Int. Ed.* **2022**, *61*, e202210123; e) H.-Y. Jang, *Org. Biomol. Chem.* **2021**, *19*, 8656-8686; f) Z. Yang, Y. Shi, Z. Zhan, H. Zhang, H. Xing, R. Lu, Y. Zhang, M. Guan, Y. Wu, *ChemElectroChem* **2018**, *5*, 3619-3623.
- [2] a) M. T. Jensen, M. H. Rønne, A. K. Ravn, R. W. Juhl, D. U. Nielsen, X.-M. Hu, S. U. Pedersen, K. Daasbjerg, T. Skrydstrup, *Nat. Commun.* **2017**, *8*, 489; b) J.-i. Yoshida, K. Kataoka, R. Horcajada, A. Nagaki, *Chem. Rev.* **2008**, *108*, 2265-2299; c) X. Peng, L. Zeng, D. Wang, Z. Liu, Y. Li, Z. Li, B. Yang, L. Lei, L. Dai, Y. Hou, *Chem. Soc. Rev.* **2023**, *52*, 2193-2237; d) J. Y. T. Kim, C. Sellers, S. Hao, T. P. Senftle, H. Wang, *Nat. Catal.* **2023**, *6*, 1115-1124.

- [3] a) L. F. T. Novaes, J. Liu, Y. Shen, L. Lu, J. M. Meinhardt, S. Lin, *Chem. Soc. Rev.* **2021**, *50*, 7941-8002; b) S. Tang, Y. Liu, L. Li, X. Ren, J. Li, G. Yang, H. Li, B. Yuan, *Org. Biomol. Chem.* **2019**, *17*, 1370-1374.
- [4] a) K. D. Moeller, *Chem. Rev.* **2018**, *118*, 4817-4833; b) C. Zhu, N. W. J. Ang, T. H. Meyer, Y. Qiu, L. Ackermann, *ACS Central Science* **2021**, *7*, 415-431; c) F. Peng, J. Xiang, H. Qin, B. Chen, R. Duan, W. Zhao, S. Liu, T. Wu, W. Yuan, Q. Li, J. Li, X. Kang, B. Han, *J. Am. Chem. Soc.* **2023**, *145*, 23905-23909; d) P. Xiong, H.-C. Xu, *Acc. Chem. Res.* **2019**, *52*, 3339-3350; e) K.-J. Jiao, Y.-K. Xing, Q.-L. Yang, H. Qiu, T.-S. Mei, *Acc. Chem. Res.* **2020**, *53*, 300-310; f) Y. Qiu, M. Stangier, T. H. Meyer, J. C. A. Oliveira, L. Ackermann, *Angew. Chem. Int. Ed.* **2018**, *57*, 14179-14183.
- [5] a) K. Yamamoto, M. Kuriyama, O. Onomura, *Acc. Chem. Res.* **2020**, *53*, 105-120; b) S. Aslam, N. Sbei, S. Rani, M. Saad, A. Fatima, N. Ahmed, *ACS Omega* **2023**, *8*, 6175-6217; c) P. Chakraborty, R. Mandal, N. Garg, B. Sundararaju, *Coord. Chem. Rev.* **2021**, *444*, 214065; d) K. Mitsudo, Y. Tachibana, E. Sato, S. Suga, *Org. Lett.* **2022**, *24*, 8547-8552; e) S. P. Blum, T. Karakaya, D. Schollmeyer, A. Klapars, S. R. Waldvogel, *Angew. Chem. Int. Ed.* **2021**, *60*, 5056-5062.
- [6] a) C. Ma, P. Fang, Z.-R. Liu, S.-S. Xu, K. Xu, X. Cheng, A. Lei, H.-C. Xu, C. Zeng, T.-S. Mei, *Science Bulletin* **2021**, *66*, 2412-2429; b) R. Francke, R. D. Little, *Chem. Soc. Rev.* **2014**, *43*, 2492-2521; c) Z. Ye, X. Zhang, W. Ma, F. Zhang, *Green Chem.* **2023**, *25*, 2524-2540.
- [7] a) G. Liu, Y. Chen, Y. Chen, Y. Shi, M. Zhang, G. Shen, P. Qi, J. Li, D. Ma, F. Yu, X. Huang, *Adv. Mater.* **2023**, *35*, 2304716; b) Z. N. Gafurov, A. O. Kanyukov, A. A. Kagilev, O. G. Sinyashin, D. G. Yakhvarov, *Coord. Chem. Rev.* **2021**, *442*, 213986; c) C. Zhu, D. Wu, H. Liu, C. Meng, T. Tang, *Green Chem.* **2022**, *24*, 9033-9039; d) X.-M. Li, Y. Wang, Y. Mu, J. Gao, L. Zeng, *J. Mater. Chem. A* **2022**, *10*, 18592-18597.
- [8] a) M. Lu, M. Zhang, J. Liu, Y. Chen, J.-P. Liao, M.-Y. Yang, Y.-P. Cai, S.-L. Li, Y.-Q. Lan, *Angew. Chem. Int. Ed.* **2022**, *61*, e202200003; b) R. Liu, K. T. Tan, Y. Gong, Y. Chen, Z. Li, S. Xie, T. He, Z. Lu, H. Yang, D. Jiang, *Chem. Soc. Rev.* **2021**, *50*, 120-242; c) D.-G. Wang, T. Qiu, W. Guo, Z. Liang, H. Tabassum, D. Xia, R. Zou, *Energy Environ. Sci.* **2021**, *14*, 688-728; d) A. P. Côté, A. I. Benin, N. W. Ockwig, M. O'Keeffe, A. J. Matzger, O. M. Yaghi, *Science* **2005**, *310*, 1166-1170; e) N. Keller, T. Bein, *Chem. Soc. Rev.* **2021**, *50*, 1813-1845; f) X. Zhao, P. Pachfule, A. Thomas, *Chem. Soc. Rev.* **2021**, *50*, 6871-6913; g) C. Yuan, Z. Wang, W. Xiong, Z. Huang, Y. Lai, S. Fu, J. Dong, A. Duan, X. Hou, L.-M. Yuan, Y. Cui, *J. Am. Chem. Soc.* **2023**, *145*, 18956-18967; h) X. Han, C. Yuan, B. Hou, L. Liu, H. Li, Y. Liu, Y. Cui, *Chem. Soc. Rev.* **2020**, *49*, 6248-6272; i) B. Han, X. Ding, B. Yu, H. Wu, W. Zhou, W. Liu, C. Wei, B. Chen, D. Qi, H. Wang, K. Wang, Y. Chen, B. Chen, J. Jiang, *J. Am. Chem. Soc.* **2021**, *143*, 7104-7113.
- [9] K. Geng, T. He, R. Liu, S. Dalapati, K. T. Tan, Z. Li, S. Tao, Y. Gong, Q. Jiang, D. Jiang, *Chem. Rev.* **2020**, *120*, 8814-8933.
- [10] C. Yuan, S. Fu, X. Kang, C. Cheng, C. Jiang, Y. Liu, Y. Cui, *J. Am. Chem. Soc.* **2023**.
- [11] Y.-R. Wang, H.-M. Ding, X.-Y. Ma, M. Liu, Y.-L. Yang, Y. Chen, S.-L. Li, Y.-Q. Lan, *Angew. Chem. Int. Ed.* **2022**, *61*, e202114648.
- [12] S. Kandambeth, K. Dey, R. Banerjee, *J. Am. Chem. Soc.* **2019**, *141*, 1807-1822.
- [13] Y.-R. Wang, M. Liu, G.-K. Gao, Y.-L. Yang, R.-X. Yang, H.-M. Ding, Y. Chen, S.-L. Li, Y.-Q. Lan, *Angew. Chem. Int. Ed.* **2021**, *60*, 21952-21958.
- [14] Y.-R. Wang, H.-M. Ding, S.-N. Sun, J.-w. Shi, Y.-L. Yang, Q. Li, Y. Chen, S.-L. Li, Y.-Q. Lan, *Angew. Chem. Int. Ed.* **2022**, *61*, e202212162.
- [15] Y. Zang, R. Wang, P.-P. Shao, X. Feng, S. Wang, S.-Q. Zang, T. C. W. Mak, *J. Mater. Chem. A* **2020**, *8*, 25094-25100.
- [16] a) T. Lu, F. Chen, *J. Comput. Chem.* **2012**, *33*, 580-592; b) T. Lu, Q. Chen, *J. Comput. Chem.* **2022**, *43*, 539-555; c) G. W. T. H. B. S. G. E. S. M. J. Frisch, J. R. C. G. S. V. B. M. A. Robb, H. N. X. L. M. C. A. V. M. G. A. Petersson, B. G. J. R. G. B. M. H. P. H. J. Bloino, A. F. I. J. L. S. D. W.-Y. J. V. Ortiz, F. L. F. E. J. G. B. P. A. P. F. Ding, D. R. V. G. Z. J. G. N. R. T. Henderson, W. L. M. H. M. E. K. T. R. F. G. Zheng, M. I. T. N. Y. H. O. K. H. N. J. Hasegawa, K. T. J. A. M. J. J. E. P. T. Vreven, M. J. B. J. J. H. E. N. B. K. N. K. F. Ogliaro, T. A. K. R. K. J. N. V. N. Staroverov, A. P. R. J. C. B. S. S. I. K. Raghavachari, M. C. J. M. M. M. K. C. A. R. C. J. Tomasi, R. L. M. K. M. O. F. J. W. Ochterski, J. B. Foresman, D. J. Fox, **2019**.



## Entry for the Table of Contents



A solid-liquid-gas three-phase indirect electrolysis system has been developed based on a covalent organic framework (Dha-COF-Cu) as heterogeneous redox mediator for S-S coupling reaction.